Environmental Science and Pollution Research (2021) 28:14957–14968
https://doi.org/10.1007/s11356-020-11719-7

RESEARCH ARTICLE

Recycling of bottom ash derived from combustion of cattle manure and its adsorption behaviors for Cd(II), Cu(II), Pb(II), and Ni(II)

Seung-Hee Hong[1] · Myung-Chul Shin[2] · Jechan Lee[3,4] · Chang-Gu Lee[3] · Dae-Sung Song[5] · Byung-Hwan Um[6] · Seong-Jik Park[7]

Received: 24 August 2020 / Accepted: 16 November 2020 / Published online: 21 November 2020

Abstract

Bottom ash generated by the combustion of cattle manure (BA-CCM) was investigated as an adsorbent for the removal of heavy metals such as Cd(II), Cu(II), Pb(II), and Ni(II) from aqueous solutions. When cattle manure was used as fuel, the thermal efficiency of the boiler was 88.7%, and the CO and CO_2 concentrations in the exhaust gas were 2.3 ppm and 12.1%, respectively. The percentage of remaining solids was 31 wt.% after combustion at 900 °C. X-ray fluorescence analyses showed that the elemental composition of the BA-CCM was mainly CaO (43.3%), SiO_2 (15.8%), CO_2 (13.0%), and P_2O_5 (10.3%). The kinetic adsorption of Cd(II), Cu(II), Pb(II), and Ni(II) by BA-CCM reached equilibrium after 12 h, and the pseudo-second-order model fitted the experimental data well. The maximum amount of Cd(II), Cu(II), Pb(II), and Ni(II) adsorbed by the bottom ash was 5.4, 72.6, 88.2, and 24.6 mg/g, respectively. The equilibrium adsorption of metals onto BA-CCM was well-described by the Freundlich model. Thermodynamic analysis showed that the adsorption onto the bottom ash was endothermic and that the Gibbs free energy decreased as the temperature increased. The presence of cations such as Na^+, Ca^{2+}, and Al^{3+} was found to reduce the amount of metals adsorbed onto the BA-CCM, and Cd(II) adsorption was found to be more dependent on ionic strength than adsorption of Cu(II), Pb(II), and Ni(II). This study demonstrates the feasibility of producing heat energy by burning cattle manure and removing heavy metals from aqueous solutions using the generated bottom ash as an adsorbent.

Keywords Cattle manure · Combustion · Bottom ash · Heavy metals · Recycling · Adsorption

Introduction

The health of soil and the environment is under increasing threat as various types of dissolved heavy metals enter and are accumulated in rivers and along coasts (Mishra et al. 2019; Wang et al. 2016). Cd, Cu, Ni, Pb, and other metals can accumulate easily in water bodies, and they are very harmful to humans if they exceed permissible levels (Mohmand et al. 2015). Metal ions are not biodegradable, and their mobility and toxicity in natural aquatic ecosystems can lead to serious health problems (Ali et al. 2019; Rota et al. 2018). Cd can cause kidney damage and renal disorders and is considered carcinogenic in humans (Chen et al. 2020a). The consumption of Cu leads to liver damage, Wilson's disease, and insomnia (Chen et al. 2020b). Pb poisoning causes anemia and nerve paralysis (Rehman et al. 2017). The effects of Ni exposure include pulmonary fibrosis and skin dermatitis (Ahmad et al. 2019). Therefore, it is important to treat toxic metals in wastewater to reduce human exposure (Zhu et al. 2020). In 2019, the Korean government set new standards for

Responsible Editor: Tito Roberto Cadaval Jr

✉ Seong-Jik Park
parkseongjik@hknu.ac.kr

[1] Department of Integrated System Engineering, Hankyong National University, Anseong 17579, Republic of Korea

[2] Department of clean energy, Korea Institute of Industrial Technology, Cheonan 31056, Republic of Korea

[3] Department of Environmental and Safety Engineering, Ajou University, Suwon 16499, Republic of Korea

[4] Department of Energy Systems Research, Ajou University, Suwon 16499, Republic of Korea

[5] Department of Water Quality & Safety Research, K-water, Daejeon 34350, Republic of Korea

[6] School of Food Biotechnology and Chemical Engineering, Hankyong National University, Anseong 17579, Republic of Korea

[7] School of Social Safety and System Engineering, Hankyong National University, Anseong 17579, Republic of Korea

heavy metal discharge into public water bodies via wastewater with maximum concentrations of Cd, Cu, Pb, and Ni of 0.1, 3.0, 0.5, and 3.0 mg/L, respectively.

Various conventional methods have been developed for the removal of heavy metal ions from aqueous solutions including ion exchange, chemical precipitation, reduction, evaporation, membrane filtration, reverse osmosis, electrodialysis, and adsorption (Mittal et al. 2016; Ahmad et al. 2017). Among the various methods used for the removal of heavy metals, adsorption is preferable because it is inexpensive and easy to implement while being highly efficient for the removal of heavy meals and producing less toxic by-products (Anastopoulos et al. 2018; Vu et al. 2019). The removal efficiency and cost of the adsorption process depend on the adsorbent used; therefore, there has been significant interest in the utilization of bottom ash as an adsorbent for the removal of heavy metals from wastewater and acid mine drainage (Asokbunyarat et al. 2015, 2017; Chiang et al. 2012; Vu et al. 2019). Bottom ash has several advantages as an adsorbent, with physical properties such as a coarse particle size, large specific surface area, and high porosity. It is also inexpensive and allows the recycling of resources (Asokbunyarat et al. 2015). However, fly ash and bottom ash produced by the incineration of coal and municipal solid waste can contain several heavy metals that can leach out under acidic conditions (Asokbunyarat et al. 2015; Shim et al. 2003).

A report by the Korean Ministry of Environment in 2017 stated that the amount of livestock manure generated in Korea was 176,434 t/d, with cattle manure accounting for 34.4% of the total. Intensive feeding in modern animal husbandry produces a large amount of cattle manure, which can easily be collected. The severe threat posed by the large quantity of cattle manure in terms of environmental greenhouse gas emissions, soil and water pollution, acidification, odor pollution, and eutrophication can be changed into a great opportunity for bioenergy generation (Zhang et al. 2020; Zhou et al. 2019). Cattle manure has a high calorific value similar to that of sawdust and rice straw (Huang et al. 2019) and a low ash content (Zhang et al. 2020). Biomass such as livestock manure is considered to be a CO_2-neutral fuel that is expected to gradually replace fossil fuels (Song et al. 2020).

Several studies have investigated the removal of heavy metals using bottom ash; however, to the best of our knowledge, bottom ash generated by the combustion of cattle manure (BA-CCM) has never been investigated. In this study, we examined the feasibility of using cattle manure as a fuel and the recycling of BA-CCM as an adsorbent for the removal of heavy metals from aqueous solutions. The physical and chemical characteristics of BA-CCM were identified by investigating its surface morphology, pore size, specific surface area, elemental composition, and crystalline structure. The adsorption characteristics of Cd(II), Cu(II), Pb(II), and Ni(II) by BA-CCM were investigated by performing batch experiments and mathematical model analysis under different reaction times, initial concentrations, and reaction temperatures. A mixed solution of Cd(II), Cu(II), Pb(II), and Ni(II) was reacted with BA-CCM at different adsorbent dosages and in the presence of competitive cations.

Materials and methods

Boiler system used to create BA-CCM

A smoke tube boiler (Kyuwon Tech Co., South Korea) with a rated thermal capacity of 230 kW (Fig. 1) is used to create BA-CCM by using cattle manure pellets as fuel to heat water (lower heating value: 2720 kcal/kg). The combustion chamber in the boiler, with a heat transfer area of 32.48 m^2, was set at a temperature of 1016.4 °C and was operated for more than 1 h. The rate at which water was supplied and the water storage capacity were 3416 kg/h and 3620 L, respectively. The boiler consumed 88.27 kg/h of cattle manure pellets as fuel.

Characterization of BA-CCM

Several analyses were conducted to characterize the BA-CCM and to investigate the mechanism by which the heavy metals were adsorbed onto the BA-CCM. The surface morphology of the BA-CCM was investigated using a field emission scanning electron microscope (FE-SEM) (S-4700, Hitachi, Japan), and the chemical composition was analyzed using an X-ray fluorescence (XRF) spectrometer (XRF-1700, Shimadzu, Japan). N_2 adsorption–desorption experiments were performed to measure the specific surface area of the BA-CCM using a surface area analyzer (Quadrasorb SI, Quantachrome Instruments, USA), and the specific surface area was determined via Brunauer–Emmett–Teller analysis. The mineralogical structures of the BA-CCM were investigated via the patterns produced during X-ray diffraction (XRD) (SmartLab, Rigaku, Japan).

Reagents and the adsorption experiment

A metal solution was prepared using $Cd(NO_3)_2{\cdot}4H_2O$, $Cu(NO_3)_2{\cdot}3H_2O$, $Pb(NO_3)_2$, and $Ni(NO_3)_2{\cdot}6H_2O$ purchased from Daejung Chemical Company (Republic of Korea). A 1000 mg/L mixed metal solution was prepared by mixing the four heavy metal reagents in distilled water. The pH of the mixed metal solution was adjusted to 4 using 0.1 mol/L of NaOH and HCl. After the adsorption reaction, the heavy metal solution was separated from the adsorbent using filter paper (0.45-μm polypropylene filter; Whatman, USA). The filtered

Fig. 1 Picture of the water heating boiler used in this study

samples were then diluted and measured with an inductively coupled plasma spectrometer (ICP-OES 5100 Series, Agilent Technologies Inc., USA). The BA-CCM was rinsed three times with distilled water and sieved to produce particles of uniform size ranging from 0.85 to 1.18 mm for the adsorption experiments.

The metal adsorption experiments using BA-CCM were performed in a batch system under various experimental conditions. The kinetic adsorption experiments were performed by varying the reaction times from 0.25 to 24 h while reacting 0.1 g of BA-CCM with 1000 mg/L of heavy metal solution at a reaction temperature of 25 °C. A shaking incubator (SJ-808SF, Sejong Scientific Co., Korea) was used to maintain the temperature and agitate the adsorbents and solutions. Equilibrium adsorption experiments were performed with different initial concentrations (5, 10, 20, 50, 100, 200, 500, and 1000 mg/L) of the heavy metal solution. The thermodynamic adsorption experiments were performed at 15, 25, and 35 °C. The dosing amount of BA-CCM was increased up to 16.7 g/L to obtain 100% removal of Cu(II) and Pb(II), and the adsorption experiments were performed under different BA-CCM dosages by varying equidistant interval (3.3, 6.7, 10.0, 13.3, and 16.7 g/L). To determine the influence of competitive cations such as Na^+, Ca^{2+}, and Al^{3+}, experiments were performed by preparing two different solutions with 1 and 10 mM of NaCl, $CaCl_2$, and $AlCl_3$. All the batch experiments were performed in triplicate.

Data analysis

The kinetic data were analyzed using the following pseudo-first-order (PFO) and pseudo-second-order (PSO) models:

$$q_t = q_e\left(1-e^{-k_1 t}\right) \tag{1}$$

$$q_t = \frac{k_2 q_e^2 t}{1 + k_2 q_e t} \tag{2}$$

where q_t is the amount of heavy metals removed at time t (mg/g), q_e is the amount of heavy metals removed at equilibrium (mg/g), k_1 is the PFO rate constant (1/h), and k_2 is the PSO rate constant (g/(mg·h)).

The equilibrium data were analyzed using the Langmuir (Eq. (3)) and Freundlich (Eq. (4)) models, as follows:

$$q_e = \frac{Q_m K_L C}{1 + K_L C} \tag{3}$$

$$q_e = K_F C_e^{\frac{1}{n}} \tag{4}$$

where C is the concentration of a heavy metal in the aqueous solution at equilibrium (mg/g); K_L is the Langmuir constant, which is related to the binding energy (L/mg); Q_m is the maximum mass of heavy metals removed per unit mass of BA-CCM (the removal capacity of BA-CCM) (mg/g); K_F is the distribution coefficient ((mg/g)·(L/mg)$^{1/n}$); and $1/n$ is a heterogeneity factor. The values of K_L, Q_m, K_F, and n can be determined by fitting the Langmuir and Freundlich models to the observed data.

The thermodynamic properties of the experimental results were analyzed using the following equations:

$$\Delta G^0 = \Delta H^0 - T\Delta S^0 \tag{5}$$

$$\Delta G^0 = -RT\ln K_e \tag{6}$$

$$\ln K_e = \frac{\Delta S^0}{R} - \frac{\Delta H^0}{RT} \tag{7}$$

$$K_e = \frac{\alpha q_e}{C_e} \quad (8)$$

where ΔG^0 is the change in Gibbs free energy (kJ/mol), ΔS^0 is the change in entropy (J/(mol·K)), ΔH^0 is the change in enthalpy (kJ/mol), K_e is the equilibrium constant (dimensionless), a is the amount of adsorbent (g/L), R is the gas constant (8.314 J/K·mol), and T is the absolute temperature (K).

Results and discussion

Combustion characteristics of cattle manure

The boiler efficiency and exhaust gas analysis results are listed in Table 1. The thermal efficiency of the boiler was estimated to be 88.7% while consuming cattle manure pellets at a rate of 33.4 kg/h. The O_2, CO, CO_2, and NO_x concentrations in the exhaust gas were 7.6%, 2.3 ppm, 12.1%, and 318 ppm, respectively, at an exhaust gas temperature of 177 °C. The concentration of pollutants emitted by the cattle manure pellet-fired boiler were compared with those produced by a firewood-fired boiler, the results of which were reported in a previous study (Vitázek et al. 2016). As shown in Fig. 2, the cattle manure pellet-fired boiler used in this study emitted less CO but more CO_2 than the firewood-fired boiler. This indicated that more complete combustion was achieved when the cattle manure pellets were used. Although the combustion of cattle-manure emitted more CO_2 (a greenhouse gas) than the combustion of firewood, it still emitted less CO_2 than a combustion of coal (Hu et al. 2000). Thus, the use of the cattle manure pellet as the solid fuel could be more environmentally beneficial than fossil fuels (e.g., coal). The combustion of cattle manure led to higher NO_x emissions than those of firewood combustion. This was likely because complete combustion leads to an increase in the formation of NO_x (i.e., thermal NO_x) (Turns 2000).

To further investigate the combustion characteristics of the cattle manure, thermogravimetric analysis (TGA) of the cattle manure was conducted in air. The thermogram (TG) and differential TG curves obtained from the TGA are presented in Fig. 3. As shown in the TG curve, four distinctive thermal degradation zones were observed. The first zone from 30 to 120 °C was due to the evaporation of water. In the second zone, approximately 23.3 wt.% of the cattle manure was thermally degraded between temperatures of 120 and 350 °C. One of the highest thermal degradation rates was measured in this zone at approximately 300 °C. Cellulose, hemicellulose, starch, and protein were combusted in the second zone (Wu et al. 2012). Lignin was combusted in the third zone between 350 and 600 °C (Wang et al. 2011). The fourth zone, which was between 600 and 900 °C, was associated with the combustion of char. Any solids that remained following the TGA (approximately 31 wt.% of the initial sample) were in the form of ash (i.e., BA-CCM).

Table 1 Efficiency and exhaust gas concentration of the cattle manure pellet-fired boiler

Boiler		Exhaust gas	
Pellet amount (kg/h)	33.4	Temperature (°C)	177.0
Input water temperature (°C)	19.2	O_2 (%)	7.6
Output water temperature (°C)	81.6	CO (ppm)	2.3
Combustion temperature (°C)	1016.4	CO_2 (%)	12.1
Efficiency (%)	88.7	NO_x (ppm)	318.0

Characterization of the BA-CCM

The physical and chemical properties of the BA-CCM were characterized by investigating the surface morphology, size, volume, specific surface area, and crystalline structure of the pores and the elemental composition of the ash. The surface morphology of the BA-CCM is obtained using FE-SEM; it consists of rod-like crystals, as shown in Fig. 4, which have also been found in bottom ash by other researchers (Chiang et al. 2012). The porous structure and rough surface composed of irregularly shaped particles contributed to the higher specific surface area of the BA-CCM (Chen et al. 2016). As shown in Table 2, the pore size and specific surface area of the BA-CCM are 15.12 nm and 1.87 m^2/g, respectively. The pores were grouped according to the definition given by the International Union of Pure and Applied Chemistry, in which adsorbent pores are classified into three groups, namely micropores (diameter < 2 nm), mesopores (2 nm < diameter < 50 nm), and macropores (diameter > 50 nm) (Wu et al. 2005). Based on this classification, the BA-CCM was composed of solids with a relatively small external surface area interspersed with multiple mesopores.

The BA-CCM was found to have a high pH of 11.8, which is considered sufficiently high to remove Cd(II), Cu(II), Pb(II), and Ni(II) via precipitation (Schneider et al. 2001). The high pH of the BA-CCM could be attributed to its alkaline nature, which resulted from high CaO contents of up to 43.3%. High CaO contents have also been observed in bottom ash by other researchers (Asokbunyarat et al. 2015).

The elemental composition of the BA-CCM generated using XRF is presented in Table 2. The BA-CCM was mainly composed of CaO, SiO_2, CO_2, and P_2O_5 with small amounts (< 5%) of other elements. Vassilev et al. (2017) reported that ash generated by the combustion of biomass mainly includes alkali metals (Na and K), alkaline earth metals (Ca and Mg),

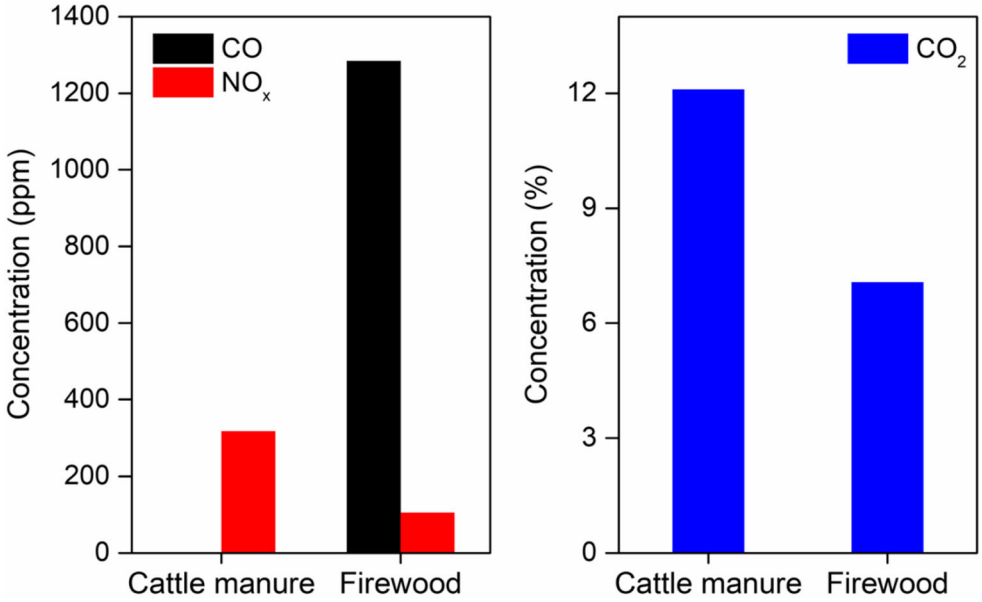

Fig. 2 Comparison of pollutants emitted from the cattle manure pellet-fired boiler with those emitted from a firewood-fired boiler reported in the literature (Vitázek et al. 2016)

Si, S, Cl, and P. The high content of alkali metals in the ash obtained from biomass combustion can reduce the heat transfer and increase the boiler tube corrosion (Tan and Lagerkvist 2011). However, because of the high CaO content, which is the main component of bottom ash, BA-CCM may be a good candidate for the removal of heavy metals in the form of insoluble hydroxides from alkaline environments (Barnes et al. 1981). The valuable nutrients P_2O_5 and K_2O were found in the BA-CCM, which implied that BA-CCM can also be used as a source of nutrients. The crystalline structure of the BA-CCM is observed by XRD analysis (Fig. 5). The presence of SiO_2, $CaCO_3$, $CaSO_4$, and $Na_6Al_6Si_{10}O_{32}$ was attributed to the high Ca and Si contents in the BA-CCM. Any K present in the ash was mainly in the form of KCl.

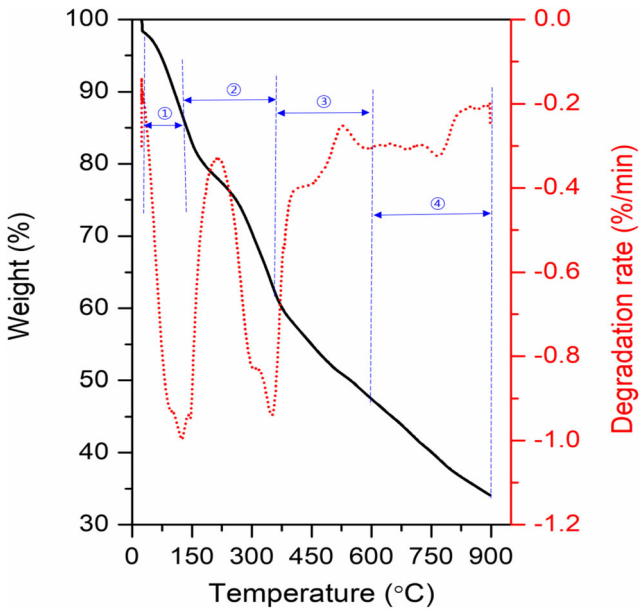

Fig. 3 Thermogram and differential thermogram obtained via thermogravimetric analysis of cattle manure pellets between 30 and 900 °C, which were heated in air at a rate of 20 °C/min

Kinetic, isotherm, and thermodynamic studies

The heavy metal adsorption by the BA-CCM depending on the reaction time is shown in Fig. 6. Cd(II), Cu(II), Pb(II), and Ni(II) were rapidly adsorbed onto the BA-CCM within 6 h, and equilibrium was reached at 12 h. The parameter values calculated using the PFO and PSO models are presented in Table 3. The equilibrium concentrations (q_e) of Cd(II), Cu(II), Pb(II), and Ni(II) that were estimated using the PSO model were higher than those estimated using the PFO model and were also closer to the observed data. The higher determination coefficient (R^2) of the PSO model also verified that the PSO model is more suitable for describing the removal of Cd(II), Cu(II), Pb(II), and Ni(II) by BA-CCM. This indicated that the rates at which Cd(II), Cu(II), Pb(II), and Ni(II) are adsorbed onto BA-CCM depend on chemisorption (Bulut et al. 2008). The reaction rates of the PFO model followed the decreasing order of Cd(II) > Pb(II) > Cu(II) > Ni(II), which was the opposite to that found using the PSO model, thereby indicating that the kinetic data are consistent.

The adsorption isotherm of BA-CCM depending on the initial metal concentrations is shown in Fig. 7. The data were fitted using the Langmuir and Freundlich models to investigate the mechanism by which metals are adsorbed onto BA-CCM. The adsorption parameters associated with the two isotherm models are shown in Table 4. The low R^2 of both models for Cd(II) and Ni(II) indicates that both Langmuir and Freundlich models were not well-fitted to Cd(II) and Ni(II) adsorption by BA-CCM. The poor fit of both models

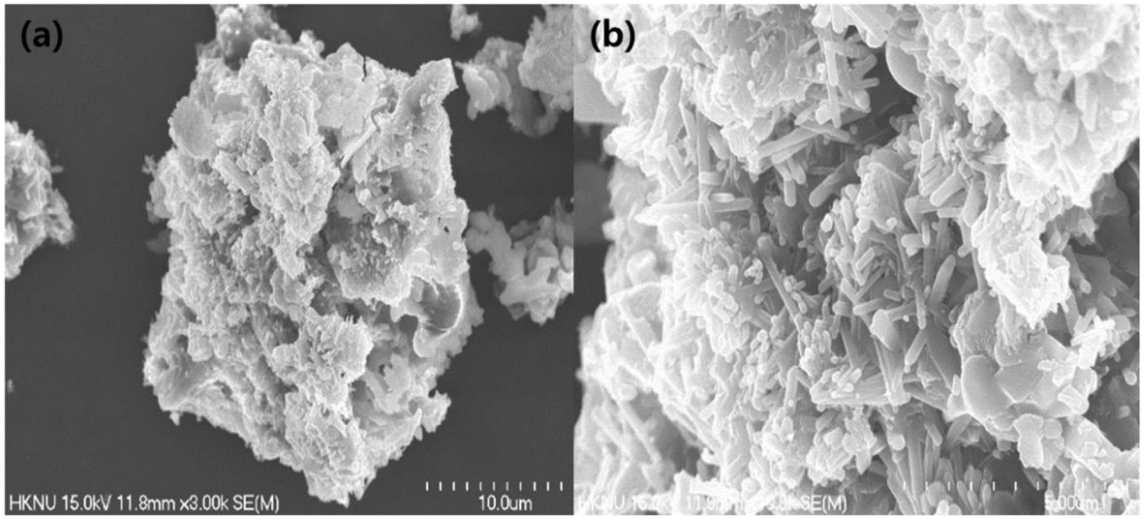

Fig. 4 Field emission scanning electron microscope image of bottom ash under (**a**) × 3000 and (**b**) × 10,000× magnification. Scale bar: (**a**) 10 μm and (**b**) 5 μm

to Cd(II) and Ni(II) adsorption was because the adsorbed amount was sharply increased in the low initial concentration. The R^2 of the Freundlich model was higher than that of the Langmuir model, which indicates that the Freundlich isotherm is more applicable for the adsorption of Cu(II) and Pb(II) onto BA-CCM. This result implies that the adsorption of Cu(II) and Pb(II) by BA-CCM was multilayer, rather than single-layer adsorption (Hui et al. 2005).

The observed maximum adsorption amounts of BA-CCM for Cd(II), Cu(II), Pb(II), and Ni(II) were 5.7 mg/g (= 0.051 mM), 73.9 mg/g (= 1.162 mM), 102.3 mg/g (= 0.494 mM), and 23.6 mg/g (= 0.402 mM), respectively. The distribution coefficients (K_F), which are related to the adsorption capacity of an adsorbent for an adsorbate, were in the order of Pb(II) > Cu(II) > Ni(II) > Cd(II) in the Freundlich model. The affinity of these heavy metals for BA-CCM can be explained by the electronegativity of metals, the hydrolysis constant, hydration energy, and the charge-to-radius ratio, and these characteristics of four ions are provided in Table 5. Electronegativity is considered to be a significant factor that influences the chemisorption of trace metals because metals with higher electronegativities can form stronger covalent bonds with O atoms on the edges of clay minerals (McBride 1994). The electronegativities of the four heavy metals in decreasing order are Pb (2.33) > Ni (1.91) > Cu (1.90) > Cd (1.69) (McBride 1994; Shi et al. 2009). Cd(II) had the lowest adsorption, which was consistent with the lowest electronegativity of Cd(II); however, Cu(II), which has a lower electronegativity than Ni(II), showed higher adsorption than Ni(II). The adsorption of metals onto adsorbents increases as the hydrolysis constant (pK) decreases. The pK of the metals in ascending order is Cu (pK = 7.7) = Pb (pK = 7.7) < Ni (pK = 9.9) < Cd (pK = 10.1) (Alloway 1995). Although Cu and Pb have the same pK, more Cu(II) than Pb(II) was adsorbed onto the BA-CCM, which was because the ionic radius of Cu (73 pm) is smaller than that of Pb (118 pm) (Marcus 1994). Cu(II), which has a smaller ionic radius, can achieve a higher Coulombic attraction toward the surface of an adsorbent than Pb(II), which has a larger ionic radius. In addition, it is difficult for ions with larger hydrated radii to enter the pores of adsorbents and undergo cation exchange at available sites (Shim et al. 2003). Cations with lower hydration bind to a greater extent than those with high hydration energy (Liu et al. 2003; Huang et al. 2012). It was expected that Ni(II) and Cu(II) with higher hydration energy would be adsorbed by BA-CCM less than Cd(II) and Pb(II). However, Cu(II) with the highest hydration energy showed the highest adsorption among the four metals tested in this study. The adsorption

Table 2 Physical properties obtained using Brunauer–Emmett–Teller analysis and the elemental composition obtained using X-ray fluorescence (XRF) analysis

Physical properties			Chemical properties									
Surface area (m^2/g)	Pore volume (cm^3/g)	Pore size (nm)	pH	XRF result (%)								
				CaO	SiO_2	CO_2	P_2O_5	Na_2O	Al_2O_3	K_2O	Fe_2O_3	Others
1.87	0.0074	15.12	11.8	43.3	15.8	13.0	10.3	3.4	3.1	3.1	1.9	6.1

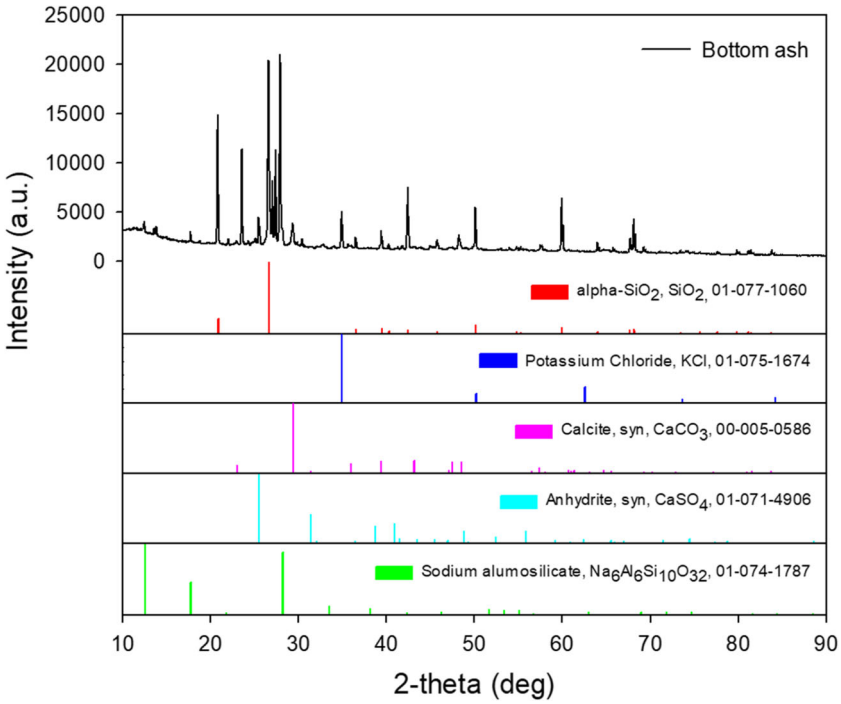

Fig. 5 X-ray diffraction patterns of bottom ash generated by the combustion of cattle manure and characteristic peaks of the identified minerals

of Cd(II), Cu(II), Pb(II), and Ni(II) by BA-CCM could not be explained solely by electronegativity, metal hydrolysis, the electrostatic force, or hydration energy; the mobility of the metals was affected by a combination of these factors (Kang et al. 2016).

The maximum adsorption (Q_m) of Cd(II), Cu(II), Pb(II), and Ni(II) by BA-CCM, which were obtained from Langmuir model fits, was 5.4, 72.6, 88.2, and 24.6 mg/g, respectively. To compare the metal adsorption capacity of BA-CCM with that of other adsorbents derived from bottom ash and fly ash, the amount of metals adsorbed by other adsorbents in the literature is provided in Table 6 in decreasing order of Cu adsorption. The adsorption of Pb(II) and Cu(II) was higher than that of Cd(II) and Ni(II), which has been observed in other studies, as mentioned previously. Of the results reported in Table 6, three adsorbents are reported to have a higher metal adsorption capacity than that of the BA-CCM used in this study. However, BA-CCM is considered to be a more effective adsorbent for the removal of heavy metals because of its low cost and its status as a by-product of cattle

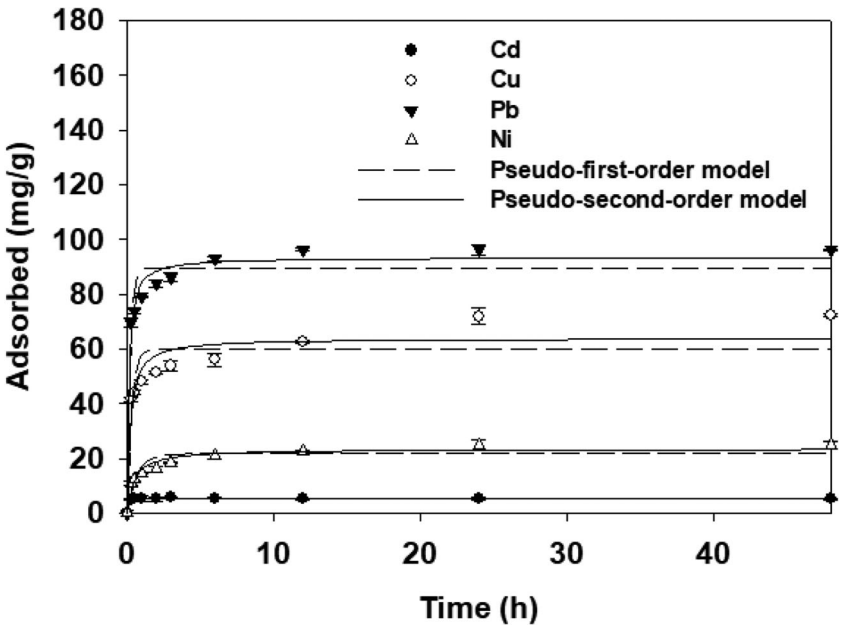

Fig. 6 Data from the kinetic adsorption experiment fitted to the pseudo-first-order and pseudo-second-order kinetic models describing the adsorption of Cd(II), Cu(II), Pb(II), and Ni(II) onto bottom ash generated by the combustion of cattle manure (BA-CCM)

Table 3 Kinetic model parameters obtained from fitting the model to the experimental data

Models		Metals			
		Cd(II)	Cu(II)	Pb(II)	Ni(II)
Pseudo-first-order kinetic model	q_e (mg/g)	5.3	59.8	89.7	21.8
	k_1 (1/h)	11.17	3.39	4.97	1.46
	R^2	0.991	0.842	0.947	0.861
Pseudo-second-order kinetic model	q_e (mg/g)	5.3	63.9	93.5	23.5
	k_2 (g/mg/h)	0.017	0.215	0.113	0.492
	R^2	0.995	0.914	0.983	0.948

manure combustion. The adsorbents that have a higher adsorption capacity than BA-CCM are not pure bottom ash but rather materials that have been synthesized from bottom ash or fly ash. The higher adsorption capacity of the other adsorbents could be a result of a high pH because it is well-known that the mobility of Cd(II), Cu(II), Pb(II), and Ni(II) decreases as a result of precipitation at a high pH (McBride 1994). Although the three adsorbents with a superior adsorption capacity are small, BA-CCM has a granular size of 0.85–1.18 mm, which enables the adsorbent to be easily separated from the solution after metal removal. Furthermore, in contrast to bottom ash derived from coal and municipal solid waste, BA-CCM does not contain heavy metals.

The thermodynamic parameters obtained from the thermodynamic analysis using Eqs. (5), (6), (7), and (8) are presented in Table 7. The amount of metal adsorption increased as the reaction temperature increased. The ΔH^0 values of Cd(II), Cu(II), Pb(II), and Ni(II) were positive, thereby indicating that the adsorption of heavy metals onto the BA-CCM was endothermic. The ΔS^0 values of Cd(II), Cu(II), Pb(II), and Ni(II) were 223.0, 145.2, 101.6, and 88.2 J/(K·mol), respectively, thereby indicating that the level of disorder at the solid–liquid interface increased during adsorption. The positive sign of ΔG^0 for Cd(II) and Ni(II) indicated that adsorption was not spontaneous under the experimental conditions in this study. The negative ΔG^0 value for Pb(II) indicated that the adsorption of Pb(II) onto the BA-CCM was spontaneous, and the change in the sign of ΔG^0 for Cu(II) at 25 °C resulted in a spontaneous reaction as the temperature increased from 15 to 25 °C.

Effects of the BA-CCM dose, competing anions, and pH

The effects of different amounts of adsorbent on the adsorption reaction with the metal solution (Cd(II), Cu(II), Pb(II),

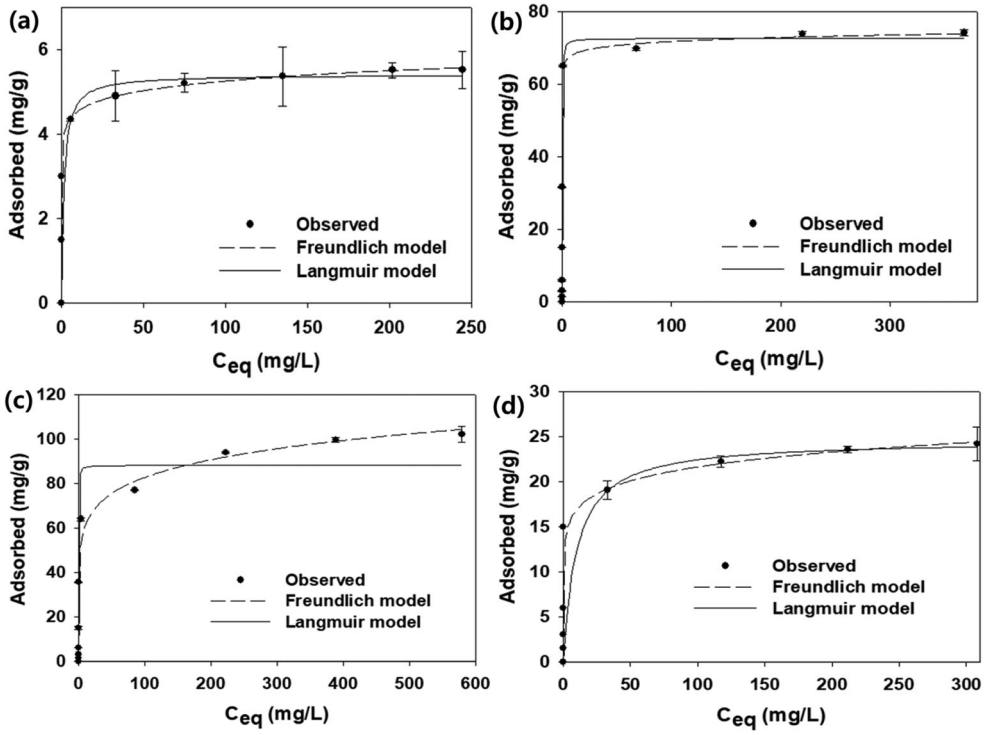

Fig. 7 Data from the equilibrium adsorption experiment fitted to the Freundlich and Langmuir isotherms for the adsorption of (**a**) Cd(II), (**b**) Cu(II), (**c**) Pb(II), and (**d**) Ni(II) onto bottom ash generated by the combustion of cattle manure (BA-CCM)

Table 4 Equilibrium model parameters obtained by fitting the model to the experimental data

Models		Parameters			
		Cd(II)	Cu(II)	Pb(II)	Ni(II)
Freundlich model	K_F ((mg/g)·(L/mg)$^{1/n}$)	3.9	64.8	45.0	13.2
	$1/n$	15.67	44.84	7.56	9.35
	R^2	0.650	0.870	0.977	0.665
Langmuir model	Q_m (mg/g)	5.4	72.6	88.2	24.6
	K_L (L/mg)	1.44	0.11	0.11	9.84
	R^2	0.646	0.869	0.933	0.665

Table 5 Electronegativity, hydrolysis constant, ionic radius, and hydration energy of Cd(II), Cu(II), Pb(II), and Ni(II)

	Electronegativity [a]	Hydrolysis constant (pK) [b]	Ionic radius (pm) [c]	Hydration energy (−ΔG, kJ/mol) [c]
Cd(II)	1.69	10.1	95	1755
Cu(II)	1.90	7.7	73	2010
Pb(II)	2.33	7.7	118	1425
Ni(II)	1.91	9.9	69	1980

[a] The electronegativity of the metals was obtained from McBride (1994)

[b] The hydrolysis constant (pK) was obtained from Alloway (1995)

[c] The ionic radius and the hydration energy were obtained from Marcus (1994)

Table 6 Comparison of the maximum metal adsorption capacity of bottom ash generated by the combustion of cattle manure (BA-CCM) with that of other adsorbents

Adsorbents	Conditions		Q_m (mg/g)				Reference
	pH	Granular size (mm)	Cd(II)	Cu(II)	Pb(II)	Ni(II)	
BA-CCM	4.0	0.850–1.180	5.40	72.60	88.2	24.60	Current research
Activated carbon-zeolite composite prepared from coal fly ash	6.7–10.0		161.90	109.20	549.1	70.40	Jha et al. 2008
Mesoporous molecular sieve synthesized from coal bottom ash	5.0	< 0.075	84.00	78.70	200.2		Vu et al. 2019
Synthesized zeolite from coal fly ash	4.0–5.0			76.90	194.7		Nascimento et al. 2009
Coal fly ash prepared zeolite	3.0–4.0	0.002		50.45		8.96	Hui et al. 2005
Incineration bottom ash	3.0–4.0	< 0.212	12.80	23.40	67.6		Wang et al. 2016
Barley straw ash	6.5	0.015–0.045	1.42	17.80		8.25	Arshadi et al. 2014
Coal bottom ash	4.2	0.300–0.700		13.40			Asokbunyarat et al. 2015
Fly ash	6.0	< 0.075		1.35		0.48	Bayat 2002
Bottom ash from a power plant	6.0	0.177	12.05				Sukpreabprom et al. 2014
Bottom ash from municipal solid waste	5.5	< 2.000	2.70		21.5		Chiang et al. 2012

Table 7 Thermodynamic parameters for the adsorption of Cd(II), Cu(II), Pb(II), and Ni(II) onto bottom ash generated by the combustion of cattle manure

Parameters	Cd(II)	Cu(II)	Pb(II)	Ni(II)
ΔH^0 (kJ/mol)	69.7	43.0	29.2	30.7
ΔS^0 (J/(K·mol))	223.0	145.2	101.6	88.2
ΔG^0 at 15 °C (kJ/mol)	5.41	1.12	− 0.04	5.33
ΔG^0 at 25 °C (kJ/mol)	3.18	− 0.33	− 1.06	4.45
ΔG^0 at 35 °C (kJ/mol)	0.95	− 1.78	− 2.07	3.57

and Ni(II)) are shown in Fig. 8a. Increasing the dose of the adsorbent from 3.33 to 16.66 g/L in the metal solution led to a decrease in the unit adsorption of Cd(II), Cu(II), Pb(II), and Ni(II). More surface functional groups and greater surface areas are available at higher adsorbent concentrations (Zhai et al. 2004). When the adsorbent dosage was increased from 3.33 to 16.66 g/L, the unit adsorption of Cd(II) decreased from 5.52 to 2.59 mg/g, while the removal percentage increased from 6.6 to 16.4%. The unit adsorption of Cu(II) decreased from 69.4 to 47.1 mg/g, while the removal percentage increased from 29.4 to 99.9%. The unit adsorption of Pb(II) decreased from 102.3 to 55.2 mg/g, while the removal percentage increased from 37.1 to 99.9%. The unit adsorption of Ni(II) decreased from 17.9 to 10.1 mg/g, while the removal percentage increased from 9.6 to 28.3%. The removal efficiency of Cu(II) and Pb(II) was approximately 90% when 13.33 g/L of BA-CCM was used as an adsorbent in the aqueous solution.

The effects of the presence of cations such as Na^+, Ca^{2+}, and Al^{3+} on the adsorption of metals by BA-CCM are presented in Fig. 8b. The amount of metals adsorbed onto the BA-CCM decreased in the presence of Na^+, Ca^{2+}, and Al^{3+}, with the impacts of these cations increasing in the order of $Na^+ < Ca^{2+} < Al^{3+}$. The reduction in the amount of metals adsorbed owing to the presence of Al^{3+} was greater than that of Na^+ because Al^{3+} can bond more strongly with the adsorbents via electrostatic attraction than Na^+ can via coulombic attraction. The electronegativities of Na^+, Ca^{2+}, and Al^{3+} are 0.93, 1.00, and 1.61, respectively, and Al^{3+}, with the highest electronegativity, is more likely to be adsorbed onto the O atoms on the edges of clay minerals via covalent bonding (McBride 1994; Mustafa et al. 2010).

Although the presence of Na^+, Ca^{2+}, and Al^{3+} reduced the metal adsorption, the differences in Cu(II), Pb(II), and Ni(II) adsorption with 1 and 10 mM of Na^+, Ca^{2+}, and Al^{3+} were not significant. However, the adsorption of Cd(II) decreased by 27.4% in the presence of 1 mM NaCl and by 86.0% in the presence of 10 mM $AlCl_3$, thereby indicating that Cd(II) adsorption is highly dependent on ionic strength. Ion adsorption by inner-sphere surface complexes showed little dependence on ionic strength, whereas the opposite was found for outer-sphere complexes (Li et al. 2006; McBride 1997). Therefore, it could be inferred that Cu(II), Ni(II), and Pb(II) were mainly adsorbed onto the BA-CCM via inner-sphere surface complexes. The adsorption of heavy metals such as Cu(II), Ni(II), and Pb(II) onto the edge sites of oxides has previously been reported to involve inner-sphere surface complexation (Gu and Evans 2008).

The effect of pH on the adsorption of heavy metals in BA-CCM is shown in the Fig. 8c. While initial pH was increased from 1.0 to 4.0, the final pH of heavy metal solution was increased from 0.26 to 8.55. The adsorption amount of all heavy metals except Ni(II) were increased along with the pH increase. Ni adsorbed amounts were kept constant around 21.8 mg/g under pH 1–4. Lower adsorption of heavy metals

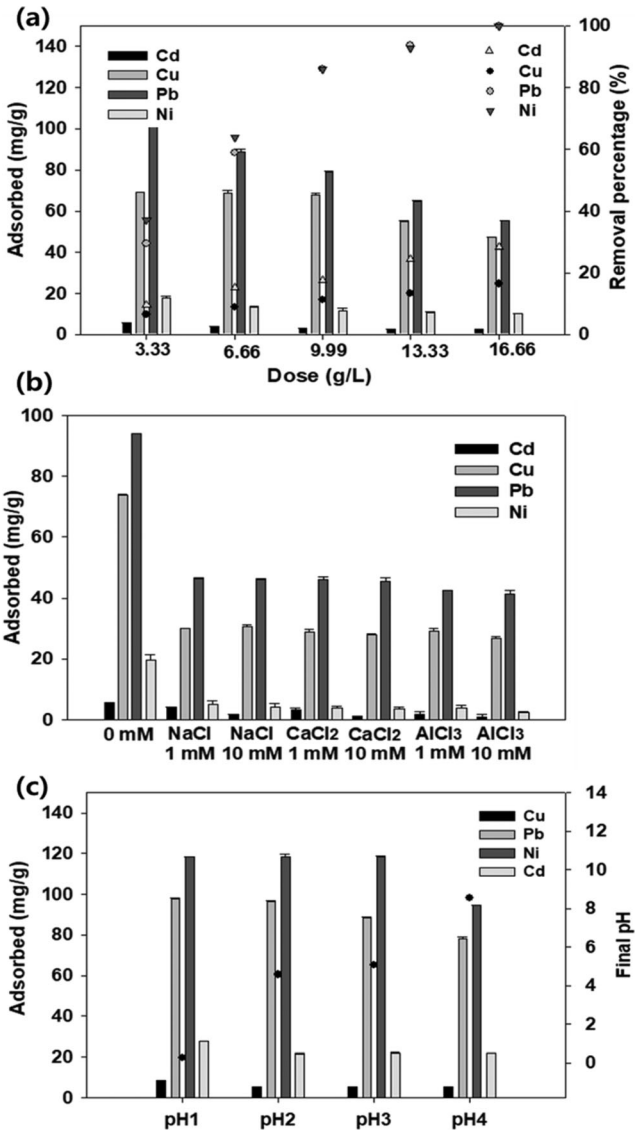

Fig. 8 Removal of heavy metals by bottom ash generated by the combustion of cattle manure (BA-CCM) under various environmental conditions: (**a**) different doses of BA-CCM, (**b**) in the presence of competitive cations (Na^+, Ca^{2+}, and Al^{3+}) at two different molar concentrations (1 and 10 mM), and (**c**) different initial solution pH (1–4)

at low pH is attributed by the protonated active sites of the adsorbent by high H^+ concentration (Mittal et al. 2016).

Conclusions

The thermal efficiency of the boiler was high when cattle manure was used as fuel, and the concentrations of CO and CO_2 in the exhaust gas from the boiler were lower than those produced by a firewood-fired boiler. In addition to the production of energy from cattle manure, the BA-CCM was used as an adsorbent for removing Cd(II), Cu(II), Pb(II), and Ni(II) from aqueous solutions. The high content of CaO in the BA-CCM led to a high pH, thereby providing favorable conditions for the removal of metals. The kinetic adsorption of Cd(II), Cu(II), Pb(II), and Ni(II) onto BA-CCM was well-described by the PSO model, thereby indicating that the rate of adsorption of the metals was mainly controlled by chemisorption. The Freundlich isotherm was more suitable for describing the adsorption of Cd(II), Cu(II), Pb(II), and Ni(II) onto the BA-CCM at equilibrium, thereby indicating that the adsorption of metals by BA-CCM was multilayered. The maximum adsorption capacity of BA-CCM for Cd(II), Cu(II), Pb(II), and Ni(II) was comparable to that of other adsorbents derived from fly ash and bottom ash in the literature, even though the results were obtained under a lower pH than that in other studies. The adsorption of metals onto BA-CCM is an endothermic reaction, and the Gibbs free energy decreased as the reaction temperature increased. More than 90% of the Cu(II) and Pb(II) could be removed via the addition of 13.33 g/L of BA-CCM. Cd(II) adsorption was highly dependent on ionic strength; however, Cu(II), Ni(II), and Pb(II) were adsorbed onto the BA-CCM via inner-sphere surface complexation. The low cost, granular size, and the absence of heavy metals are advantages of using BA-CCM as adsorbents for the removal of heavy metals. The use of combustion by-products as adsorbents is valuable in terms of recycling of resources and economics.

Authors' contributions Seung-Hee-Hong: Experiment, data analysis, writing-original draft Myung-Chul Shin: Conceptualization, data analysisJechan Lee: Partial writing-original draftChang-Gu Lee: Writing-review and editingDae-Sung Song: Data analysisByung-Hwan Um: Funding acquisitionSeong-Jik Park: Conceptualization, writing-review and editing, supervision

Funding This work was carried out with the support of the "Cooperative Research Program for Agriculture Science and Technology Development (Project No. PJ01477903)," the Rural Development Administration, Republic of Korea.

Data availability All data generated or analyzed during this study are included in this published article. The datasets used and/or analyzed during the current study are available from the corresponding author on reasonable request.

Compliance with ethical standards

Conflict of interest The authors declare that they have no conflict of interest.

Ethics approval and consent to participate Not applicable.

Consent for publication Not applicable.

Consent for participation Not applicable.

References

Ahmad R, Hasan I, Mittal A (2017) Adsorption of Cr (VI) and Cd (II) on chitosan grafted polyaniline-OMMT nanocomposite: isotherms, kinetics and thermodynamics studies. Desalin Water Treat 58:144–153

Ahmad J, Naeem S, Ahmad M, Usman AR, Al-Wabel MI (2019) A critical review on organic micropollutants contamination in wastewater and removal through carbon nanotubes. J Environ Manag 246:214–228

Ali H, Khan E, Ilahi I (2019) Environmental chemistry and ecotoxicology of hazardous heavy metals: environmental persistence, toxicity, and bioaccumulation. J Chem 2019:1–14

Alloway BJ (1995) Chapter 2. Soil processes and the behavior of heavy metals. In: Alloway BJ (ed) Heavy metals in soils, 2nd edn. Blackie Academic and Professional, London, pp 11–37

Anastopoulos I, Mittal A, Usman M, Mittal J, Yu G, Núñez-Delgado A, Kornaros M (2018) A review on halloysite-based adsorbents to remove pollutants in water and wastewater. J Mol Liq 269:855–868

Arshadi M, Amiri MJ, Mousavi S (2014) Kinetic, equilibrium and thermodynamic investigations of Ni (II), Cd (II), Cu (II) and Co (II) adsorption on barley straw ash. Water Resour Ind 6:1–17

Asokbunyarat V, van-Hullebusch ED, Lens PN, Annachhatre AP (2015) Coal bottom ash as sorbing material for Fe (II), Cu (II), Mn (II), and Zn (II) removal from aqueous solutions. Water Air Soil Pollut 226(5):143

Asokbunyarat V, van-Hullebusch ED, Lens PN, Annachhatre AP (2017) Immobilization of metal ions from acid mine drainage by coal bottom ash. Water Air Soil Pollut 228(9):328

Barnes D, Bliss PJ, Gould BW, Vallentine HR (1981) Water and wastewater engineering systems. Pitman, London; Marshfield, pp 148–150

Bayat B (2002) Comparative study of adsorption properties of Turkish fly ashes: I. the case of nickel (II), copper (II) and zinc (II). J Hazard Mater 95(3):251–273

Bulut E, Özacar M, Şengil İA (2008) Equilibrium and kinetic data and process design for adsorption of Congo red onto bentonite. J Hazard Mater 154(1–3):613–622

Chen Z, Liu Y, Zhu W, Yang EH (2016) Incinerator bottom ash (IBA) aerated geopolymer. Constr Build Mater 112:1025–1031

Chen J, He W, Zhu X, Yang S, Yu T, Ma W (2020a) Epidemiological study of kidney health in an area with high levels of soil cadmium and selenium: does selenium protect against cadmium-induced kidney injury? Sci Total Environ 698:134106

Chen C, Chen Q, Kang J, Shen J, Wang B, Guo F, Chen Z (2020b) Hydrophilic triazine-based dendron for copper and lead adsorption in aqueous systems: performance and mechanism. J Mol Liq 298:112031

Chiang YW, Ghyselbrecht K, Santos RM, Meesschaert B, Martens JA (2012) Synthesis of zeolitic-type adsorbent material from municipal

solid waste incinerator bottom ash and its application in heavy metal adsorption. Catal Today 190(1):23–30
Gu X, Evans LJ (2008) Surface complexation modelling of Cd (II), Cu (II), Ni (II), Pb (II) and Zn (II) adsorption onto kaolinite. Geochim Cosmochim Acta 72(2):267–276
Hu Y, Naito S, Kobayashi N, Hasatani M (2000) CO_2, NOx and SO_2 emissions from the combustion of coal with high oxygen concentration gases. Fuel 79(15):1925–1932
Huang KJ, Teng FZ, Wei GJ, Ma JL, Bao ZY (2012) Adsorption-and desorption-controlled magnesium isotope fractionation during extreme weathering of basalt in Hainan Island, China. Earth Planet Sci Lett 359:73–83
Huang HJ, Chang YC, Lai FY, Zhou CF, Pan ZQ, Xiao XF, Wang J, Zhou CH (2019) Co-liquefaction of sewage sludge and rice straw/wood sawdust: the effect of process parameters on the yields/properties of bio-oil and biochar products. Energy 173:140–150
Hui KS, Chao CYH, Kot SC (2005) Removal of mixed heavy metal ions in wastewater by zeolite 4A and residual products from recycled coal fly ash. J Hazard Mater 127(1–3):89–101
Jha VK, Matsuda M, Miyake M (2008) Sorption properties of the activated carbon-zeolite composite prepared from coal fly ash for Ni^{2+}, Cu^{2+}, Cd^{2+} and Pb^{2+}. J Hazard Mater 160(1):148–153
Kang K, Lee CG, Choi JW, Kim YK, Park SJ (2016) Evaluation of the use of sea sand, crushed concrete, and bentonite to stabilize trace metals and to interrupt their release from contaminated marine sediments. Water Air Soil Pollut 227(9):308
Li W, Zhang S, Jiang W, Shan XQ (2006) Effect of phosphate on the adsorption of cu and cd on natural hematite. Chemosphere 63(8):1235–1241
Liu C, Zachara JM, Smith SC, McKinley JP, Ainsworth CC (2003) Desorption kinetics of radiocesium from subsurface sediments at Hanford site, USA. Geochim Cosmochim Acta 67(16):2893–2912
Marcus Y (1994) A simple empirical model describing the thermodynamics of hydration of ions of widely varying charges, sizes, and shapes. Biophys Chem 51(2–3):111–127
McBride MB (1994) Environmental chemistry of soils. Oxford University Press, New York
McBride MB (1997) A critique of diffuse double layer models applied to colloid and surface chemistry. Clay Clay Miner 45(4):598–608
Mishra S, Bharagava RN, More N, Yadav A, Zainith S, Mani S, Chowdhary P (2019) Heavy metal contamination: an alarming threat to environment and human health. In: Environmental biotechnology: For sustainable future, pp 103–125
Mittal A, Ahmad R, Hasan I (2016) Biosorption of Pb^{2+}, Ni^{2+} and Cu^{2+} ions from aqueous solutions by L-cystein-modified montmorillonite-immobilized alginate nanocomposite. Desalin Water Treat 57(38):17790–17807
Mohmand J, Eqani SAMAS, Fasola M, Alamdar A, Mustafa I, Ali N, Liu L, Peng S, Shen H (2015) Human exposure to toxic metals via contaminated dust: bio-accumulation trends and their potential risk estimation. Chemosphere 132:142–151
Mustafa S, Shah KH, Naeem A, Ahmad T, Waseem M (2010) Counter-ion effect on the kinetics of chromium (III) sorption by Amberlyst. 15 in H^+, Li^+, Na^+, Ca^{++}, Al^{+++} forms. Desalination 264(1–2):108–114
Nascimento M, Soares PSM, de-Souza VP (2009) Adsorption of heavy metal cations using coal fly ash modified by hydrothermal method. Fuel 88(9):1714–1719
Rehman ZU, Khan S, Brusseau ML, Shah MT (2017) Lead and cadmium contamination and exposure risk assessment via consumption of vegetables grown in agricultural soils of five-selected regions of Pakistan. Chemosphere 168:1589–1596
Rota E, Bianchi N, Bargagli R (2018) Metal availability and transfer along food chains in Siena, a small medieval town in Italy. J Chem 2018:1–8
Schneider IA, Rubio J, Smith RW (2001) Biosorption of metals onto plant biomass: exchange adsorption or surface precipitation? Int J Miner Process 62(1–4):111–120
Shi T, Jia S, Chen Y, Wen Y, Du C, Guo H, Wang Z (2009) Adsorption of Pb (II), Cr (III), Cu (II), Cd (II) and Ni (II) onto a vanadium mine tailing from aqueous solution. J Hazard Mater 169(1–3):838–846
Shim YS, Kim YK, Kong SH, Rhee SW, Lee WK (2003) The adsorption characteristics of heavy metals by various particle sizes of MSWI bottom ash. J Waste Manag 23(9):851–857
Song Y, Hu J, Liu J, Evrendilek F, Buyukada M (2020) Catalytic effects of CaO, Al_2O_3, Fe_2O_3, and red mud on Pteris vittata combustion: emission, kinetic and ash conversion patterns. J Clean Prod 252:119646
Sukpreabprom H, Arquero OA, Naksata W, Sooksamiti P, Janhom S (2014) Isotherm, kinetic and thermodynamic studies on the adsorption of Cd (II) and Zn (II) ions from aqueous solutions onto bottom ash. Int J Environ Sci Dev 5(2):165
Tan Z, Lagerkvist A (2011) Phosphorus recovery from the biomass ash: a review. Renew Sust Energ Rev 15(8):3588–3602
Turns SR (2000) An introduction to combustion: concepts and applications, 2nd edn. McGraw-Hill
Vassilev SV, Vassileva CG, Song YC, Li WY, Feng J (2017) Ash contents and ash-forming elements of biomass and their significance for solid biofuel combustion. Fuel 208:377–409
Vitázek I, Klúčik J, Mikulová Z, Vereš P (2016) Effects on concentration of selected gaseous emissions at biomass combustion. AIP Conf Proc 1768:020022. https://doi.org/10.1063/1.4963044
Vu DH, Bui HB, Bui XN, An-Nguyen D, Le QT, Do NH, Nguyen H (2019) A novel approach in adsorption of heavy metal ions from aqueous solution using synthesized MCM-41 from coal bottom ash. Int J Environ Anal Chem:1–19
Wang L, Shahbazi A, Hanna MA (2011) Characterization of corn stover, distiller grains and cattle manure for thermochemical conversion. Biomass Bioenergy 35(1):171–178
Wang Y, Huang L, Lau R (2016) Conversion of municipal solid waste incineration bottom ash to sorbent material for pollutants removal from water. J Taiwan Inst Chem Eng 60:275–286
Wu FC, Tseng RL, Hu CC (2005) Comparisons of pore properties and adsorption performance of KOH-activated and steam-activated carbons. Microporous Mesoporous Mater 80(1–3):95–106
Wu H, Hanna MA, Jones DD (2012) Thermogravimetric characterization of dairy manure as pyrolysis and combustion feedstocks. Waste Manag Res 30(10):1066–1071
Zhai Y, Wei X, Zeng G, Zhang D, Chu K (2004) Study of adsorbent derived from sewage sludge for the removal of Cd^{2+}, Ni^{2+} in aqueous solutions. Sep Purif Technol 38(2):191–196
Zhang J, Sun G, Liu J, Evrendilek F, Buyukada M (2020) Co-combustion of textile dyeing sludge with cattle manure: assessment of thermal behavior, gaseous products, and ash characteristics. J Clean Prod 253:119950
Zhou S, Liang H, Han L, Huang G, Yang Z (2019) The influence of manure feedstock, slow pyrolysis, and hydrothermal temperature on manure thermochemical and combustion properties. Waste Manag 88:85–95
Zhu S, Khan MA, Wang F, Bano Z, Xia M (2020) Rapid removal of toxic metals Cu^{2+} and Pb^{2+} by amino trimethylene phosphonic acid intercalated layered double hydroxide: a combined experimental and DFT study. Chem Eng J 392:123711